2) マイクロサテライト多型の特徴と用途

マイクロサテライト多型の例は図1-1に示した。ゲノム上のユニークな配列に挟まれて，数塩基程度の単純な配列の繰り返しが見られ，その繰り返し回数の数に個人差が認められる。通常，5種類以上の対立遺伝子があり，高いヘテロ接合度（heterozygosity）を示す。すなわち大多数の人はヘテロ接合型になるので，個々のマイクロサテライト多型から得られる情報が多いのが特徴である。疾患や形質にかかわる遺伝子を探索するための連鎖解析や関連解析にしばしば使われる遺伝マーカーである。

図1-3はマイクロサテライト多型マーカーを用いた連鎖解析の例として，日本人小児喘息についての報告を示す[1]。多発家系の試料をなるべく多数収集して，ゲノム全域にほぼ均等に分布する300～400種類程度のマイクロサテライト多型マーカーを解析し，その結果から染色体上の位置ごとに疾患遺伝子の存在確率を求める。連鎖に関する統計遺伝学的手法はいくつかあるが，現在では，いずれかの連鎖解析用プログラムを用いてコンピュータ計算するのが通常である（I部3章）。この例では，疾患遺伝子が存在する可能性の高いピーク（候補領域）がいくつか見られ，特に5番染色体上のピークが高いのが分かる。

マイクロサテライト多型マーカーのもう1つの応用例を図1-4に示す[2]。骨髄移植や輸血の後に起こる副作用の1つにGVHD（移植片対宿主病）がある。これは，提供者（ドナー）の免疫担当細胞が患者の組織を非自己と認識して攻撃するもので，拒絶反応とは反対の現象である。マイクロサテライト多型マーカーによる個人識別能力を生かして，GVHDの確定診断のために，患者血液中の白血球DNAのマイクロサテライト型がドナー由来の型に換わっていることを示している。

3) SNPの特徴と用途

塩基1個の差異からなるSNPの1例は図1-2に示した。個々のSNPは対立遺伝子が2個に限られ情報量は多くない。しかしながら前述のごとく，ゲノム中の分布密度が高いため，それらの組み合わせ，すなわちSNPハプロタイプをマーカーと考えれば高度な多型性を示す。

図1-5に示したように，SNPsはその存在部位によって大別される。このうち，エクソン内にあるSNPやプロモーター領域にあって遺伝子発現量に影響するSNPなどは，イントロン部分にあるSNPや遺伝子と遺伝子の間にあるSNPより疾患感受性にかかわる可能性が高いと考えられる。

これらの疾患感受性／抵抗性遺伝子多型を見出す統計遺伝学方法についてはI部を参照いただきたい。疾患感受性遺伝子や抵抗性遺伝子を明らかにすることは，ゲノム創薬，個人化医療（personalized medicine）や新しい予防医学を実現するためにも必要である。

図1-6は，前述した喘息の連鎖解析（図1-3）によって検出された候補領域について，多数のSNPを用いた関連解析を行うことにより，疾患遺伝子を同定することができた例である[3]。一般に，連鎖解析によって検出される候補領域は広大であり，しばしば10Mb以上に及んで100個以上の遺伝子を含んでいる。この中から疾患遺伝子を特定するためには，この領域内に存在する多数のSNPについて，それらの間の連鎖不平衡を考慮しながら関連解析を行い，最も強い関連を示すSNPあるいはSNPハプロタイプを見出す必要がある（I部参照）。

図1-3 マイクロサテライト多型マーカーを用いた罹患同胞対法による連鎖解析の例：喘息，染色体1～12番の結果のみ表示

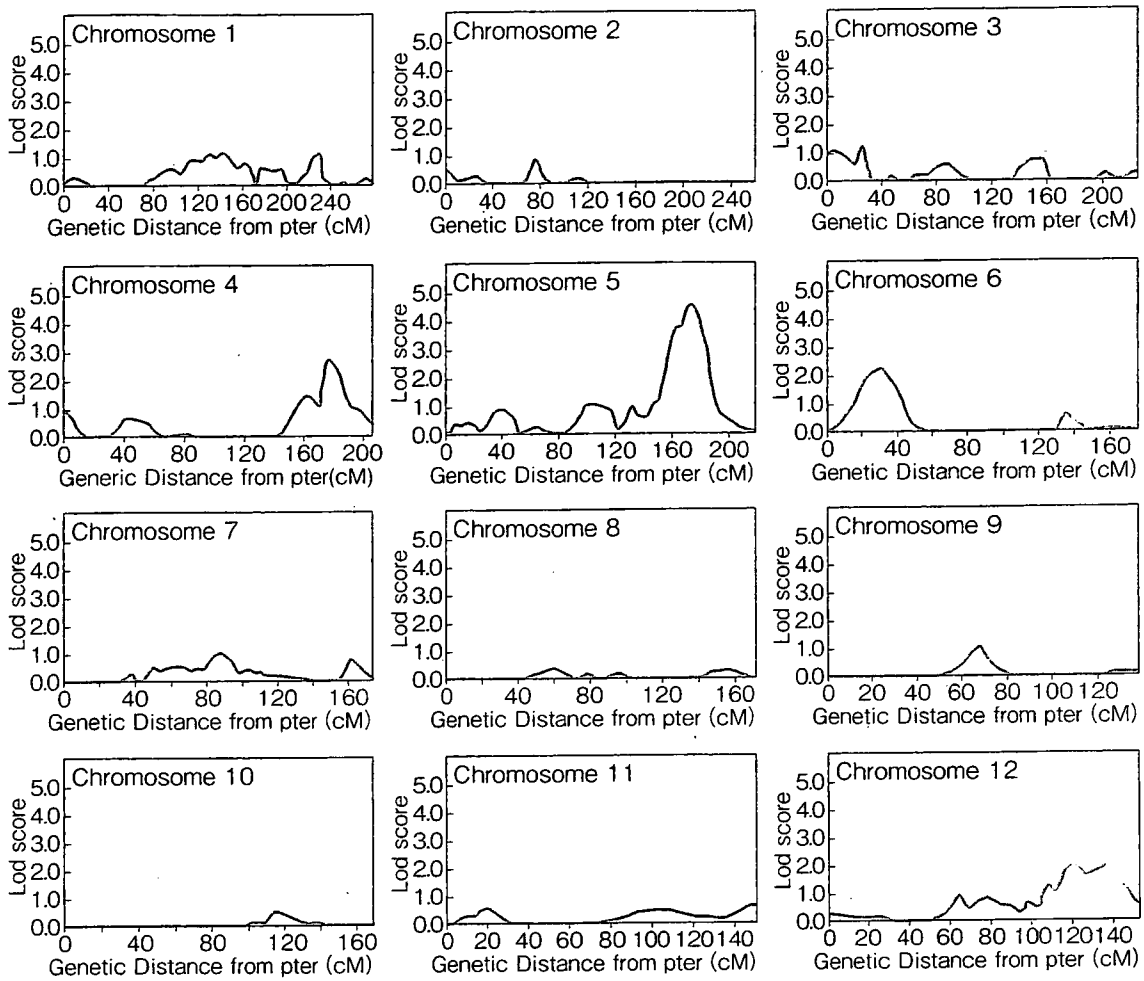

出典 参考文献1）より引用改変

図1-4 マイクロサテライト多型解析による輸血後GVHDの確定診断

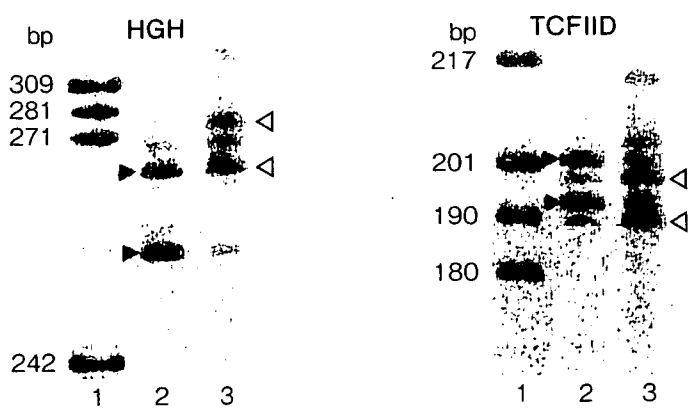

2種のマイクロサテライト多型を解析した結果。それぞれ，レーン1はサイズマーカー，レーン2は患者皮膚（患者本来の型），レーン3は患者末梢血（GVHD発症によってドナーの型が主になっている）から得られたパターン。

出典 参考文献2）より引用改変

図1-5　SNPの位置による分類

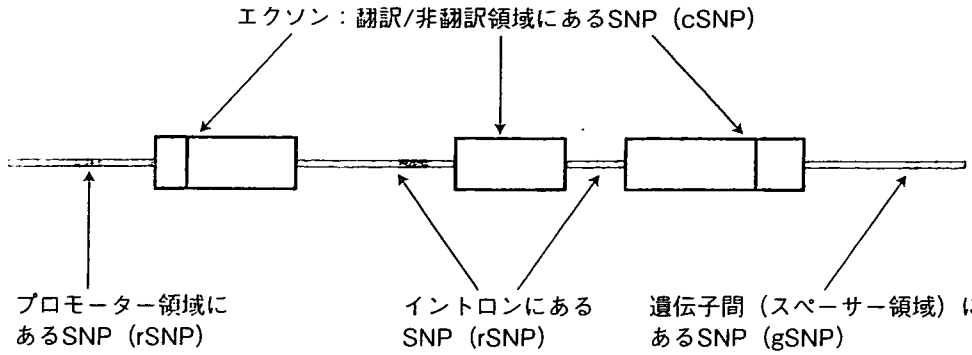

図1-6　SNPを用いた疾患遺伝子マッピングの例

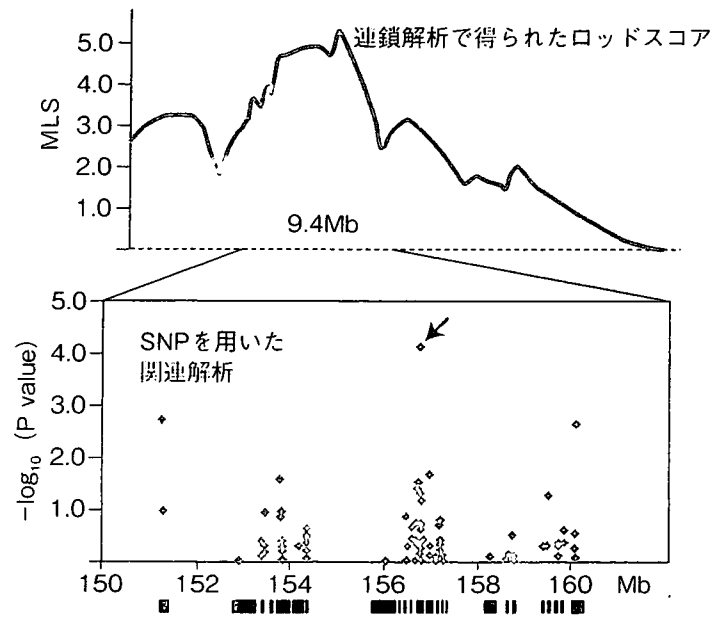

連鎖解析（図1-3参照）によって検出された5番染色体短腕上の候補領域について高密度のSNP関連解析を行った結果，矢印の位置に喘息感受性遺伝子があると推定された。

出典　参考文献3）より引用改変

2. 変異・多型の解析技術

マイクロサテライト多型の解析においては，ゲル電気泳動と銀染色を組み合わせるか，蛍光標識プライマーを用いたPCR産物を自動シークエンサーで解析する場合が多い。一方，SNP解析については，その判別原理はハイブリダイゼーション，特異的プライマー伸長など限られているものの，検出法などにはさまざまな工夫がなされ多様な技術が開発されている。最近，全ゲノム増幅技術や数十万種ものSNPsを一挙に解析する技術の発達も著しい。

1）マイクロサテライト多型の解析技術

マイクロサテライト多型の解析においては，繰り返し配列部分の両側にあるユニークな配列部分に相補的なPCRプライマーを設定する。PCR増幅断片を電気泳動してその長さを判別することにより，繰り返し回数を決定できる。先に紹介した図1-4はこの電気泳動後に銀染色を施して遺

図1-7 プール試料を用いた自動シークエンサーによるマイクロサテライトマーカーの対立遺伝子頻度推定

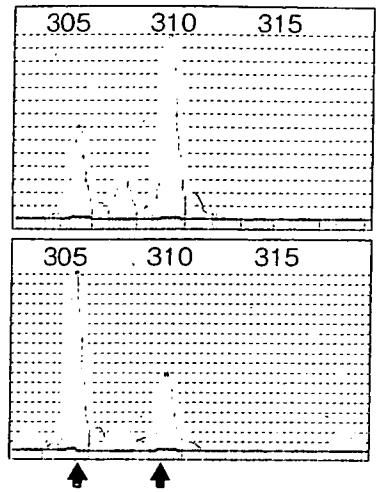

矢印の対立遺伝子については健常者と患者での頻度が異なることから，このマーカーと疾患が関連すると考えられる。

伝子型を決定した例である。一方，図1-7は多数の検体から得たゲノムDNAを等量ずつ混合したプール試料について解析した例である。蛍光プライマーを用いて標識されたPCR産物を，自動シークエンサーによって分離検出した泳動像であり，それぞれのピークの高さの相対値に基づいて各対立遺伝子の頻度を推定できる。疾患関連研究において，候補領域・遺伝子を検出するため多数のマイクロサテライト多型をスクリーニングする際に，コストや手間を省く手段として用いられることがある[4]。

2) SNP解析技術

多因子疾患感受性遺伝子や薬剤応答性遺伝子の探索研究におけるSNP解析の有用性に加えて，個人化医療の時代におけるSNP検査の重要性が指摘されており，近年のSNPタイピング技術の進歩は目覚ましい。表1-2は主な方法について，その多型判別原理や測定法に基づいて分類したものである。それぞれに特徴があり，検体数や解析したいSNPの種類数などに応じて，適切な方法を選ぶことが望ましい[5]。

Hybridizationを原理とする方法では，従来より用いられてきたナイロン膜上でのオリゴヌクレオチドプローブによるSNPタイピング法に加えて（図1-8），マイクロタイタープレートなどを支持体として用いたり，従来とは逆にプローブをあらかじめ支持体に固定しておくなどの方法が確立されている（図1-9）。さらに処理能力を増大させるため，シリコンやガラスなどの基板を支持体としてSNP特異的オリゴヌクレオチドプローブを高密度に固定化しておき，hybridizeした検体DNAを蛍光測定法や電気化学的方法によって検出する方法があり，これらを一般にDNAチップと呼ぶ。チップを用いず，液相中でFRET（fluorescence resonance energy transfer）法を用いる方法も開発されている。SNPの近傍の塩基配列はSNPごとに異なるため，多種類のSNPsを同一のhybridization-washing条件で精度良く判別することは容易ではないが，その検出段階でさまざまな工夫がなされている。

一方，hybridizationを用いるとともに，SNP自体の判別には酵素反応を組み合わせる方法と

表1-2　主なＳＮＰタイピング技術

Hybridizationを用いる
- SSO（sequence specific oligonucleotide probing）法
- DNAチップ法
- チップ—電気化学的検出法
- FRET検出法　など

Hybridizationと酵素反応の組み合わせ
- Invader法
- Sniper法　など

構造の差異を検出する
- SSCP（single strand conformation polymorphism）法
- DHPLC法　など

特異的伸長反応を検出する
- SSP（sequence specific primer）法
- MALDI-TOF/MS法
- 一分子蛍光検出法　など

塩基配列決定法を用いる

図1-8　PCR-SSO法の原理

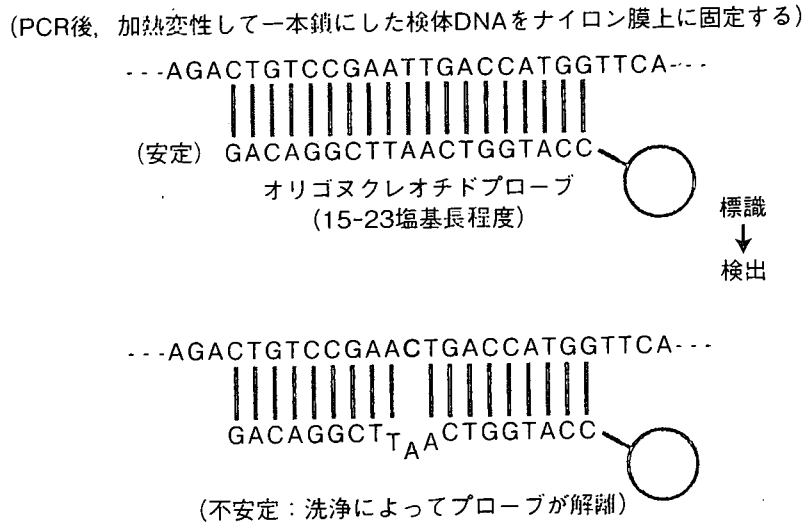

して，cleavaseとFRET測定を用いるInvader法や，ligaseとRolling circle DNA amplificationを用いるSniper法がある。どちらも大量検体のタイピングを目指す方法である。また，ビーズを支持体としてligaseを用い，プローブごとに異なる波長の蛍光を発するよう標識するLuminex法などもある。

Hybridizationを用いない方法として，DNA二本鎖あるいは一本鎖の構造の違いを検出する方法がある。特に，一本鎖DNAの構造の違いを検出するSSCP（single strand conformation polymorphism）法は比較的簡便な方法として広く用いられている。**図1-10**はその原理を図示したもので，**図1-11**はゲル電気泳動で分離後に銀染色を施したものである。近年は蛍光プライマーを

図1-9 PCR-reversed SSO法の原理

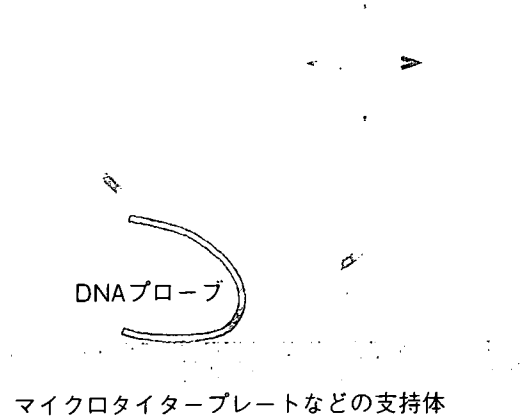

図1-10 PCR-SSCP法の原理

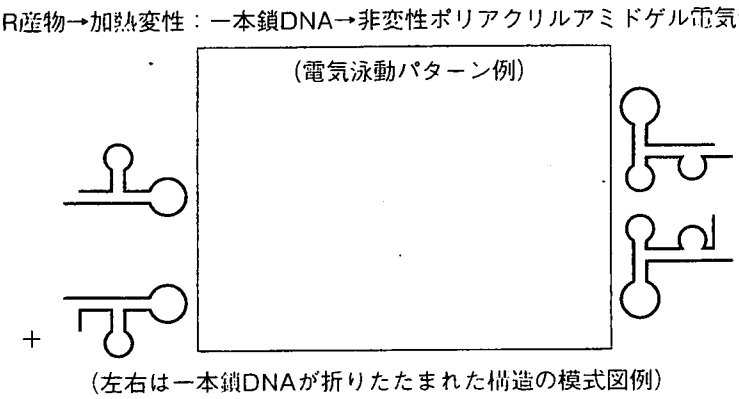

図1-11 ゲル電気泳動と銀染色を用いたPCR-SSCP法の例

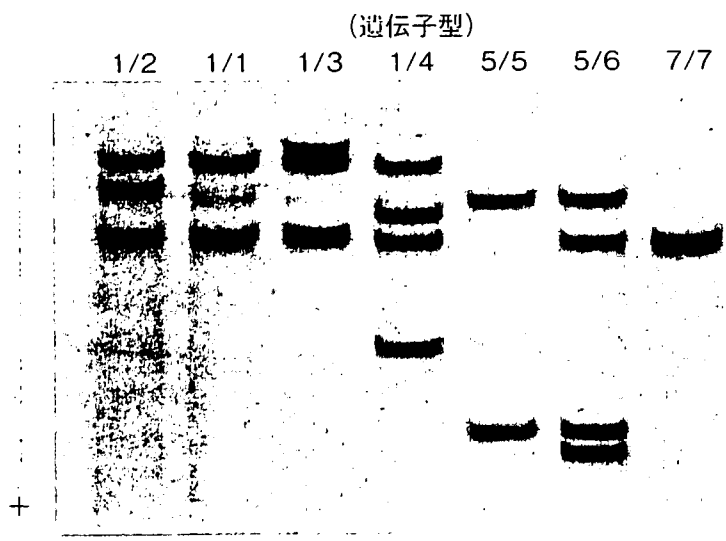

写真では多数の対立遺伝子が見られるが，SNPでは2種の対立遺伝子の組み合わせによる3種の遺伝子型が見られる。

図1-12　キャピラリー型自動シークエンサーと複数の蛍光標識プライマーを用いたPCR-SSCP法の例

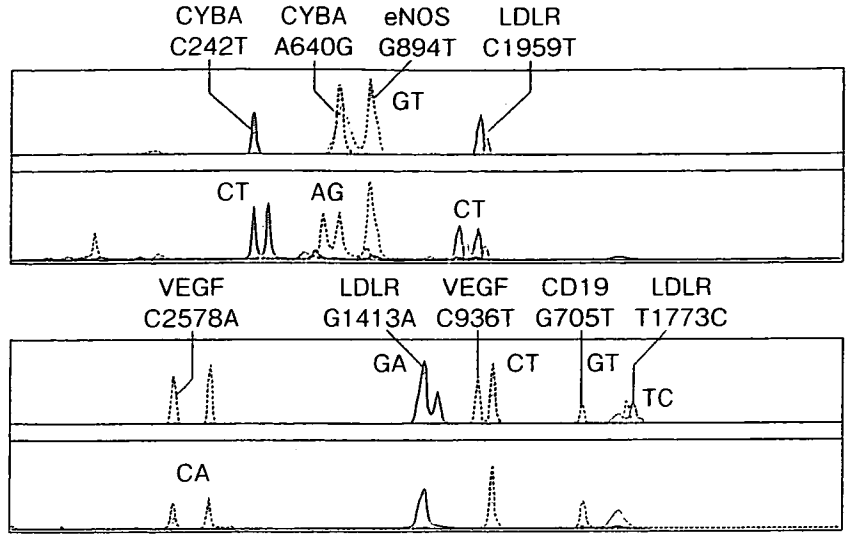

出典　参考文献7）より引用改変

図1-13　プール試料からのSNP対立遺伝子頻度推定：自動シークエンサーを用いたSSCP法の例

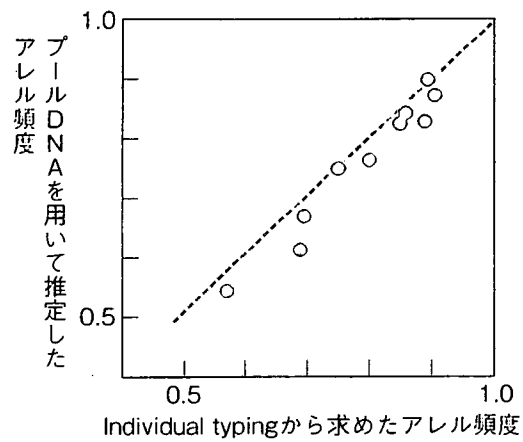

出典　参考文献7）より引用改変

用いてPCRを行った産物をキャピラリー型自動シークエンサーで解析することにより処理能力を向上する考案もなされている（図1-12）[6)7)]。多数の試料を等量ずつ混合したプール試料から，一挙にSNP対立遺伝子頻度を推定することも可能である（図1-13）[6)7)]。また，標準二本鎖DNAと検体二本鎖DNAとでheteroduplexを作らせ，これをHPLC（high performance liquid chromatography）で検出する方法も開発されている。これらは既知のSNPsのタイピングとともに，未知のSNPsの検出にも利用できる方法である。

次に，SNP特異的プライマーによる伸長反応を行わせて検出する方法がある。従来よりASP（allele specific primer）法あるいはSSP（sequence specific primer）法が広く用いられてきた（図1-14）。TaqMan法はこの特異的伸長反応とFRET測定を組み合わせた方法である。さらに，一塩基の伸長産物を検出する方法として，MALDI-TOF/MS（matrix-assisted laser desorption ionization time-of-flight mass spectrometry）法を用いる方法があり，PCR-SSP産物を検出する一分子蛍光検出法がある（図1-15，16）。

図1-14 PCR-SSP法の原理

SNP特異的なプライマーを用いたPCR伸長反応を検出する

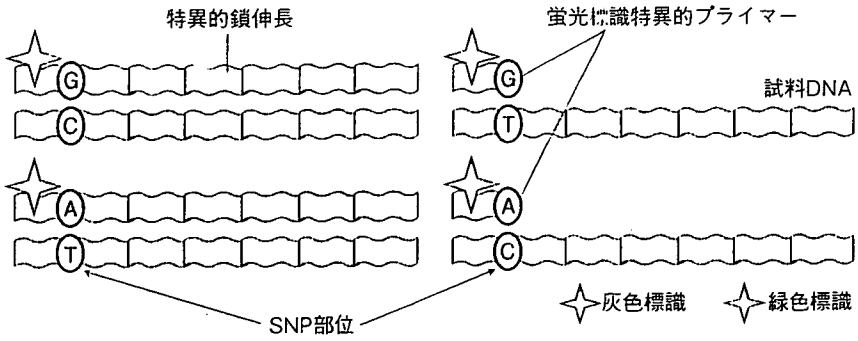

対立遺伝子C：灰色標識増幅産物が得られる
対立遺伝子T：緑色標識増幅産物が得られる

図1-15 SNP特異的PCRと一分子蛍光検出法（蛍光相関法）を組み合わせたSNPタイピング法

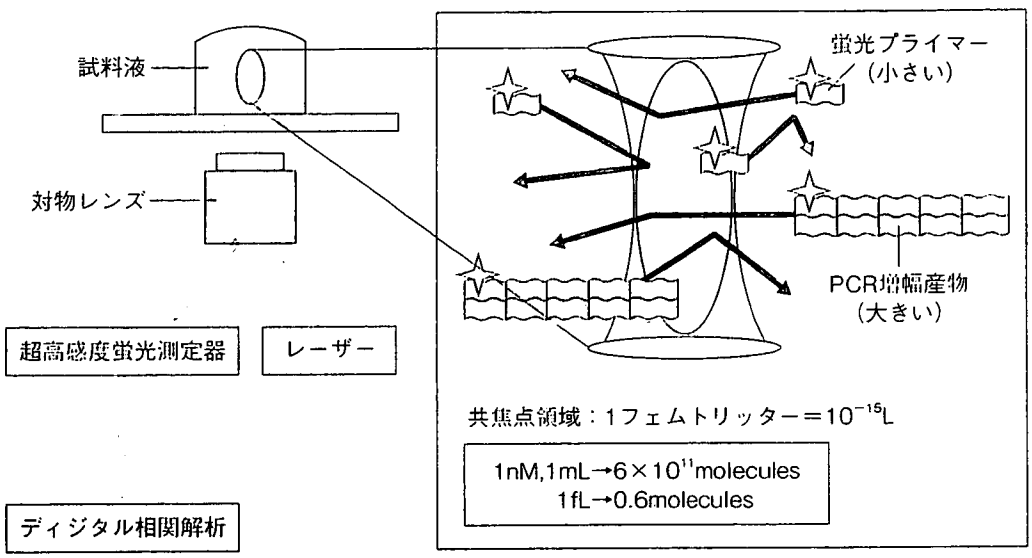

出典 参考文献8）より引用改変

図1-16 全ゲノム増幅試料を用いたSNPタイピングの例

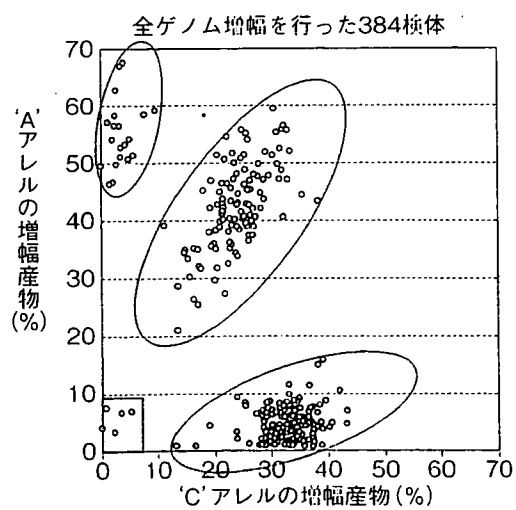

出典 参考文献8）より引用改変

後者は蛍光相関分光法（fluorescent correlation spectroscopy）を検出に用いる方法で，多数検体のタイピングに適する[8]。さらには塩基配列決定によってSNPタイピングを実行することもあるが，現状ではコストと手間がかかるため，多数検体の解析には適さない。通常のシークエンサーを用いる方法以外にも，SNPを含む30塩基以内の配列を簡便に決定するPyrosequencing法がある。

3）全ゲノム増幅技術

近年，微量あるいは保存状態の悪いゲノムDNAからゲノム全域をカバーする多量の増幅断片を生成する技術（whole genome amplification）が開発されてきた[9]。これはもともと，考古学的試料などの微量かつ損傷を受けた貴重なDNAを分析するために工夫された技術であるが，疾患関連遺伝子の探索研究において，限られた量の患者ゲノムDNAを用いて多数の遺伝子・ゲノム多型を解析する際にも有用である。PEP（primer preamplification）法とDOP（degenerate oligonucleotide primer）法が用いられてきたが，最近ではMDA（multiple displacement amplification）法が増幅効率も高く，ゲノムのほとんどの領域をほぼ同等に増幅できる方法として評価されている。筆者らの経験でもほとんどのSNPについて増幅しないゲノムDNAを用いた場合と同じ結果が得られているので，実用上の問題はない。一方，マイクロサテライト多型については，全ゲノム増幅の際に繰り返し数のずれ（slippage）が生じることがあり，増幅しないゲノムDNAを用いた場合との一致率が70％から95％程度と報告されているので，他に手段がない場合にのみ用いる方法だと考えられる。先に示した**図1-16**は全ゲノム増幅法と前述した一分子蛍光検出法を組み合わせ，384穴のマイクロタイタープレート上でSNPタイピングを行った例である[8]。3つの遺伝子型のクラスターが明瞭に分離されている。

4）大規模ゲノムワイドSNP解析技術

現在，ヒトのさまざまな多因子疾患にかかわる遺伝子を探索する戦略として最も注目を浴びているのがゲノムワイド関連解析法（genomewide association analysis）である。このためには，多数の患者，対照者試料について，ゲノム全域に分布する数十万種類のSNPを解析しなければならないが，従来の技術ではコストおよび労力が膨大であった。最近，少なくとも2つのメーカーがより実用的な技術を開発した[10) 11)]。その1つ（Affymetrix社）では，まず制限酵素反応でゲノムDNAの断片化を行い，続いてそれら断片の両端にアダプター配列を付加し，それらをまとめて増幅した後に蛍光標識を施した後に，マイクロアレイを用いたアレル特異的なハイブリダイゼーションによりSNPタイピングを行う（**図1-17**）。現在では，この方法を用いて50万種を超えるSNPを同時にタイピングするキットが市販されている。筆者らはこのキットを用いるSNP解析システムを構築し，いくつかの多因子疾患についてゲノムワイド関連解析を実施している。その1例として，睡眠障害の1つであるナルコレプシーの結果の一部を紹介する。ヒトのナルコレプシーについては，すでに確立した感受性遺伝子として，6番染色体上の*HLA-DQB1*遺伝子が知られている。**図1-18**はHLA遺伝子領域について得られた結果であるが，期待どおり*HLA-DQB1*遺伝子近傍をピークとする強い関連が認められた（宮川卓ら未発表データ）。

（徳永勝士）

図1-17 ゲノムワイド探索用SNPタイピングシステムの例

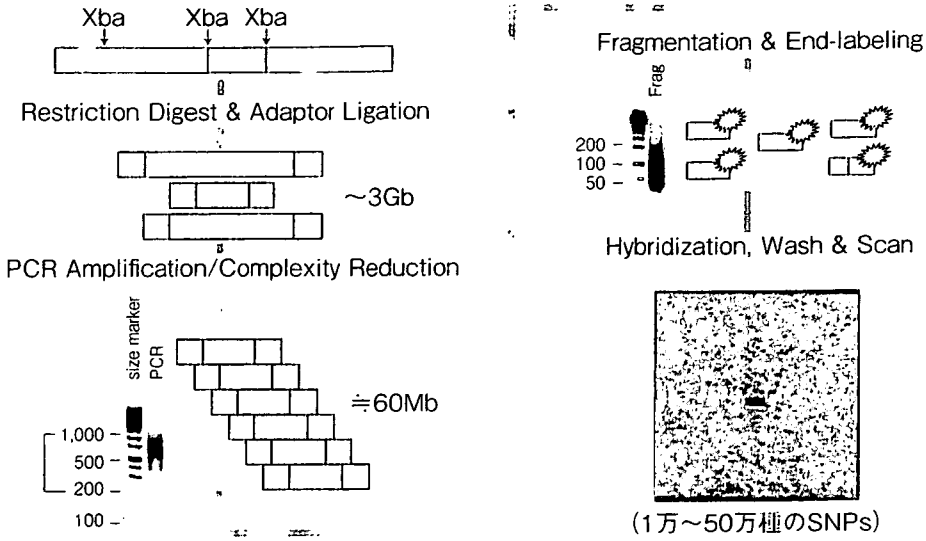

出典 参考文献10）より引用改変

図1-18 ヒトナルコレプシーにおけるHLA遺伝子領域のSNPを用いた関連解析の結果

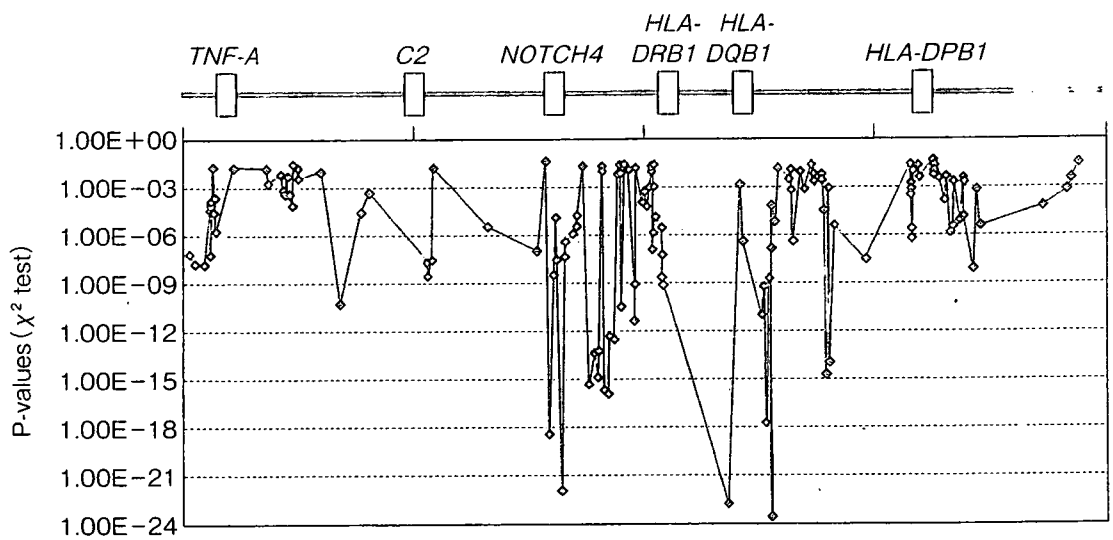

（宮川卓ら未発表データ）

1) Yokouchi Y, Nukaga Y, Shibasaki M, et al : Significant evidence for linkage of mite-sensitive childhood asthma to chromosome 5q31-q33 near the interleukin 12 B locus by a genome-wide search in Japanese families. ***Genomics*** **66** : 152-160, 2000

2) Wang L, Juji T, Tokunaga K, et al : Polymorphic microsatellite markers for the diagnosis of graft-versus-host disease. ***N Engl J Med*** **330** : 398-401, 1994

3) Noguchi E, Yokouchi Y, Zhang J, et al : Positional identification of an asthma susceptibility gene on human chromosome 5q33. ***Am J Respir Crit Care Med*** **172** : 183-188, 2005

4) Kawashima M, Tamiya G, Oka A, et al : Genome-wide association analysis of human narcolepsy and a new resistance gene. ***Am J Hum Genet*** **79** : 252-263, 2006

5) 辻本壮三, 田中利男 編：ゲノム研究実験ハンドブック. 羊土社, 東京, 2004

6) 馬場由吾, 林健志：SNPsとは何か？「ゲノム医科学がわかる」 菅野純夫 編, 羊土社, 東京, 32-39, 2001

7) Doi K, Doi H, Noiri E, et al : High-throughput single nucleotide polymorphism tying by fluorescent single-strand conformation polymorphism analysis with capillary electrophoresis. ***Electrophoresis*** **25** : 833-838, 2004

8) Bannai M, Higuchi K, Akesaka T, et al : Single-nucleotide-polymorphism genotyping for whole-genome-amplified samples using automated fluorescence correlation spectroscopy. ***Anal Biochem*** **327** : 215-221, 2004

9) Hughes S, Lasken R (eds) : Whole genome Amplification. Scion Publishing, 2005

10) Matsuzaki H, Loi H, Dong S, et al : Parallel genotyping of over 10,000 SNPs using a one-primer assay on a high-density oligonucleotide array. ***Genome Res*** **14** : 414-425, 2004

11) Oliphant A, Barker DL, Stuelpnagel JR, et al : BeadArray technology : enabling an accurate, cost-effective approach to high-throughput genotyping. ***Biotechniques*** **32** : S56-S61, 2002

0090-9556/06/3407-1229–1236$20.00
DRUG METABOLISM AND DISPOSITION
Copyright © 2006 by The American Society for Pharmacology and Experimental Therapeutics
DMD 34:1229–1236, 2006

Vol. 34, No. 7
9290/3119191
Printed in U.S.A.

DRUG-DRUG INTERACTION BETWEEN PITAVASTATIN AND VARIOUS DRUGS VIA OATP1B1

Masaru Hirano, Kazuya Maeda, Yoshihisa Shitara, and Yuichi Sugiyama

Graduate School of Pharmaceutical Sciences, the University of Tokyo, Tokyo, Japan (M.H., K.M., Y.Su.); and Graduate School of Pharmaceutical Sciences, Chiba University, Chiba, Japan (Y.Sh.)

Received January 6, 2006; accepted March 29, 2006

ABSTRACT:

It has already been demonstrated that pitavastatin, a novel potent HMG-coenzyme A reductase inhibitor, is taken up into human hepatocytes mainly by organic anion transporting polypeptide (OATP) 1B1. Because OATP2B1 is also localized in the basolateral membrane of human liver, we took two approaches to further confirm the minor contribution of OATP2B1 to the hepatic uptake of pitavastatin. Western blot analysis revealed that the ratio of the band density of OATP2B1 in human hepatocytes to that in our expression system is at least 6-fold lower compared with OATP1B1 and OATP1B3. The uptake of pitavastatin in human hepatocytes could be inhibited by both estrone-3-sulfate (OATP1B1/OATP2B1 inhibitor) and estradiol-17β-D-glucuronide (OATP1B1/OATP1B3 inhibitor). These results further supported the idea that OATP1B1 is a predominant transporter for the hepatic uptake of pitavastatin. Then, to explore the possibility of OATP1B1-mediated drug-drug interaction, we checked the inhibitory effects of various drugs on the pitavastatin uptake in OATP1B1-expressing cells and evaluated whether the in vitro inhibition was clinically significant or not. As we previously reported, we used the methodology for estimating the maximum unbound concentration of inhibitors at the inlet to the liver ($I_{u,in,max}$). Judging from $I_{u,in,max}$ and inhibition constant (K_i) for OATP1B1, several drugs (especially cyclosporin A, rifampicin, rifamycin SV, clarithromycin, and indinavir) have potentials for interacting with OATP1B1-mediated uptake of pitavastatin. The in vitro experiments could support the clinically observed drug-drug interaction between pitavastatin and cyclosporin A. These results suggest that we should pay attention to the concomitant use of some drugs with pitavastatin.

The liver is one of the organs responsible for the elimination of xenobiotics including many kinds of drugs. In some cases, although the compounds were not supposed to easily penetrate the plasma membrane from the viewpoint of their physicochemical properties, they were efficiently taken up into liver and excreted into bile. Recently, it has been found that several kinds of transporters greatly help the efficient membrane transport of several compounds. It has been characterized that hepatic uptake of some of the compounds is mediated by organic anion-transporting polypeptide (OATP) family transporters, organic anion transporter 2, Na^+-taurocholate cotransporting polypeptide, and organic cation transporter 1 (Mizuno et al., 2003). Among these transporters, especially OATP1B1 and OATP1B3 are specifically expressed in liver and show broad substrate specificities (Hagenbuch and Meier, 2003). In contrast, OATP2B1 is also expressed in the basolateral membrane of human liver (Tamai et al., 2001). Previous reports indicated that the low pH facilitates the OATP2B1-mediated uptake of several organic anions, implying its involvement in the intestinal absorption of anions (Kobayashi et al., 2003). Although the uptake clearance at pH 7.4 was lower than that at pH 5.0, OATP2B1 could transport some organic anions such as estrone-3-sulfate, fexofenadine, benzylpenicillin, and dehydroepiandrosterone sulfate, even at pH 7.4 (Kobayashi et al., 2003; Nozawa et al., 2004). Therefore, it is possible that OATP2B1 is also involved in the hepatic uptake of anionic drugs.

Pitavastatin is a highly potent inhibitor of HMG-coenzyme A reductase, the rate-limiting enzyme in cholesterol biosynthesis (Aoki et al., 1997; Kajinami et al., 2003). Previously, Kimata et al. (1998) have revealed that [^{14}C]pitavastatin is selectively distributed to the liver in rats with the liver-to-plasma concentration ratio of more than 50, suggesting that active transport systems can be involved in the uptake of pitavastatin. We have already demonstrated that pitavastatin is taken up into human hepatocytes predominantly by OATP1B1, although it was a substrate of both OATP1B1 and OATP1B3 (Hirano et al., 2004). We also showed that the contribution of other transporters such as OATP2B1 to the pitavastatin uptake was theoretically small, but we have not experimentally shown the minor importance of OATP2B1. Therefore, we tried to confirm that OATP1B1 is a responsible transporter for the pitavastatin uptake by two kinds of approaches: the comparison of the expression level of each transporter in human hepatocytes and expression systems by Western blot analysis, and the inhibitory effects of transporter-selective inhibitors on the uptake of pitavastatin in human hepatocytes.

This work was supported by Health and Labour Sciences Research Grants from the Ministry of Health, Labour and Welfare for the Research on Advanced Medical Technology and a Grant-in Aid for Young Scientists (B) (15790087) from the Ministry of Education, Culture, Sports, Science and Technology.

Article, publication date, and citation information can be found at http://dmd.aspetjournals.org.

doi:10.1124/dmd.106.009290.

ABBREVIATIONS: HEK, human embryonic kidney; MDCK, Madin-Darby canine kidney; OATP, organic anion-transporting polypeptide; HMG-CoA, 3-hydroxy-3-methylglutaryl-coenzyme A; K_m, Michaelis constant; V_{max}, maximum transport velocity; K_i, inhibition constant; $E_2$17βG, estradiol 17β-D-glucuronide; E_1S, estrone-3-sulfate; DDI, drug-drug interaction.

The combination therapy of statins and various compounds is widely used in clinical practice. Coadministration of various drugs sometimes causes an increase in the plasma concentration of statins (Williams and Feely, 2002), which may occasionally lead to severe side effects such as myopathy and rhabdomyolysis (Evans and Rees, 2002). In the case of simvastatin, which is relatively lipophilic and metabolized by CYP3A4, itraconazole, cyclosporin A, and erythromycin were reported to increase plasma area under the plasma concentration-time curve of simvastatin by inhibition of CYP3A4-mediated metabolism (Kantola et al., 1998; Neuvonen et al., 1998; Ichimaru et al., 2001). In contrast, cyclosporin A also interacted with the nonmetabolized type of statins such as pravastatin, pitavastatin, and rosuvastatin in the clinical situation (Olbricht et al., 1997; Hasunuma et al., 2003; Simonson et al., 2004). Shitara et al. (2003) clarified that drug-drug interaction (DDI) between cyclosporin A and cerivastatin is caused by the inhibition of OATP1B1-mediated cerivastatin uptake by cyclosporin A. Because pitavastatin was reported to be taken up into hepatocytes mainly by OATP1B1 (Hirano et al., 2004), we should pay attention to the OATP1B1-mediated DDI of pitavastatin in coadministration with other drugs that can inhibit the function of OATP1B1. However, the inhibitors of OATP1B1 identified by in vitro analyses do not always cause DDI in the clinical situation when the clinical protein unbound concentration in plasma is much lower than the in vitro inhibition constant (K_i) for OATP1B1. Ito et al. (1998) proposed the calculation method for estimating the maximum unbound concentration of inhibitors at the inlet to the liver to avoid the false-negative prediction of clinical DDI.

In the present study, we confirmed the minor contribution of OATP2B1 to the hepatic uptake of pitavastatin by two approaches. Moreover, we tried to predict the possible DDI mediated by OATP1B1 between pitavastatin and various drugs by judging from the clinical maximum unbound concentration of each inhibitor in human plasma and the K_i value for OATP1B1 obtained from the in vitro study.

Materials and Methods

Materials. Pitavastatin, monocalcium bis[(3*R*,5*S*,6*E*)-7-[2-cyclopropyl-4-(4-fluorophenyl)-3-quinolyl]3,5-dihydroxy-6-hepteonate], was synthesized by Nissan Chemical Industries (Chiba, Japan). [^{3}H]Pitavastatin (16.0 Ci/mmol) was synthesized by GE Healthcare (Little Chalfont, Buckinghamshire, UK). [^{3}H]Estradiol 17β-D-glucuronide ($E_2$17βG) and [^{3}H]estrone-3-sulfate (E_1S) (45 Ci/mmol and 46 Ci/mmol, respectively) were purchased from New England Nuclear (Boston, MA). Unlabeled $E_2$17βG, E_1S, and gemfibrozil were purchased from Sigma-Aldrich (St. Louis, MO). A metabolite of gemfibrozil, M3 (purity 99.6%), was chemically synthesized at KNC Laboratories, Co. Ltd. (Kobe, Japan) as shown in detail previously (Shitara et al., 2004). All other chemicals were of analytical grade and commercially available.

Uptake Study Using Transporter Expression Systems. OATP1B1-, OATP1B3-, and OATP2B1-expressing HEK293 cells and vector-transfected control cells used in this study were constructed previously (Hirano et al., 2004; Shimizu et al., 2005). Transporter-expressing or vector-transfected HEK293 cells were grown in Dulbecco's modified Eagle's medium low glucose (Invitrogen, Carlsbad, CA) supplemented with 10% fetal bovine serum (Sigma-Aldrich), 100 U/ml penicillin, 100 μg/ml streptomycin, and 0.25 μg/ml amphotericin B at 37°C with 5% CO_2 and 95% humidity. Cells were then seeded in 12-well plates coated with poly-L-lysine/poly-L-ornithine at a density of 1.5×10^5 cells per well. After 2 days, the cell culture medium was replaced with culture medium supplemented with 5 mM sodium butyrate 24 h before transport assay to induce the expression of exogenous transporters. The transport study was carried out as described previously (Sugiyama et al., 2001). Uptake was initiated by adding Krebs-Henseleit buffer containing radiolabeled and unlabeled substrates after cells had been washed twice and preincubated with Krebs-Henseleit buffer at 37°C for 15 min. The Krebs-Henseleit buffer consisted of 118 mM NaCl, 23.8 mM $NaHCO_3$, 4.8 mM KCl, 1.0 mM KH_2PO_4, 1.2 mM $MgSO_4$, 12.5 mM HEPES, 5.0 mM glucose, and 1.5 mM $CaCl_2$ adjusted to pH 7.4. The uptake was terminated at a designated time by adding ice-cold Krebs-Henseleit buffer after removal of the incubation buffer. Then, cells were washed twice with 1 ml of ice-cold Krebs-Henseleit buffer, solubilized in 500 μl of 0.2 N NaOH, and kept overnight at 4°C. Aliquots (500 μl) were transferred to scintillation vials after adding 250 μl of 0.4 N HCl. The radioactivity associated with the cells and incubation buffer was measured in a liquid scintillation counter (LS6000SE; Beckman Coulter, Inc., Fullerton, CA) after adding 2 ml of scintillation fluid (Clear-sol I; Nacalai Tesque, Kyoto, Japan) to the scintillation vials. The remaining 50 μl of cell lysate was used to determine the protein concentration by the method of Lowry et al. (1951) with bovine serum albumin as a standard.

Uptake Study Using Human Cryopreserved Hepatocytes. This experiment was performed as described previously (Shitara et al., 2003). Cryopreserved human hepatocytes were purchased from In Vitro Technologies (Baltimore, MD). In this experiment, we selected three batches of human hepatocytes (lots OCF, 094, and ETR), which ranked in the top three of the uptake amount of $E_2$17βG, and E_1S among eight independent batches of hepatocytes. Immediately before the study, the hepatocytes (1-ml suspension) were thawed at 37°C, quickly suspended in 10 ml of ice-cold Krebs-Henseleit buffer, and centrifuged (50*g*) for 2 min at 4°C, followed by removal of the supernatant. This procedure was repeated once more to remove cryopreservation buffer, and then the cells were resuspended in the same buffer to give a cell density of 1.0×10^6 viable cells/ml for the uptake study. The number of viable cells was determined by trypan blue staining. Before the uptake studies, the cell suspensions were prewarmed in an incubator at 37°C for 3 min. The uptake studies were initiated by adding an equal volume of buffer containing radiolabeled and unlabeled pitavastatin to the cell suspension. After incubation at 37°C for 0.5 and 2 min, the reaction was terminated by separating the cells from the buffer. For this purpose, an aliquot of 80 μl of incubation mixture was collected and placed in a centrifuge tube (450 μl) containing 50 μl of 2 N NaOH under a layer of 100 μl of oil (density, 1.015; a mixture of silicone oil and mineral oil; Sigma-Aldrich), and subsequently the sample tube was centrifuged for 10 s using a tabletop centrifuge (10,000*g*; Beckman Microfuge E; Beckman Coulter, Inc.). During this process, hepatocytes passed through the oil layer into the alkaline solution. After an overnight incubation in alkali to dissolve the hepatocytes, the centrifuge tube was cut and each compartment was transferred to a scintillation vial. The compartment containing the dissolved cells was neutralized with 50 μl of 2 N HCl, mixed with scintillation cocktail, and the radioactivity was measured in a liquid scintillation counter.

Antiserum and Western Blot Analysis. As shown in previous reports, anti-OATP2B1 sera were raised in rabbits against a synthetic peptide consisting of the 15 carboxyl-terminal amino acids of OATP2B1 (LLVSGPGKKPEDSRV) coupled to keyhole limpet hemocyanine at its N-terminal via an additional cysteine (Kullak-Ublick et al., 2001). Crude membrane fractions were prepared from human hepatocytes and transporter-expressing HEK293 cells as described previously (Sasaki et al., 2002). The human liver block (lot 020188) was obtained from Human and Animal Bridging Research Organization (Chiba, Japan), and crude membrane fractions were prepared as described previously (Hirano et al., 2004). The samples were diluted with 3× Red loading buffer (BioLabs, Hertfordshire, UK) and loaded onto a 7% SDS-polyacrylamide gel with a 4.4% stacking gel. Proteins were electroblotted onto a polyvinylidene difluoride membrane (Pall, East Hills, NY) using a blotter (Trans-blot; Bio-Rad, Richmond, CA) at 15 V for 1 h. The membrane was blocked with Tris-buffered saline containing 0.05% Tween 20 (TBS-T) and 5% skimmed milk for 1 h at room temperature. After washing with TBS-T, the membrane was incubated with anti-OATP2B1 serum (dilution 1:1000). The membrane was incubated with a horseradish peroxidase-labeled anti-rabbit IgG antibody (GE Healthcare) diluted 1:5000 in TBS-T for 1 h at room temperature, followed by washing with TBS-T. The band was detected and its intensity was quantified using an image analyzer (LAS-1000 plus; Fuji Film, Tokyo, Japan).

Transcellular Transport Study. OATP1B1-, OATP1B1/BCRP-, OATP1B1/MDR1-, and OATP1B1/MRP2-expressing MDCKII cells and vector-transfected control cells used in this study were constructed previously (Matsushima et al., 2005). Transporter-expressing or vector-transfected MDCKII cells were grown in Dulbecco's modified Eagle's medium low glucose supplemented with 10% fetal bovine serum, 100 U/ml penicillin, 100

μg/ml streptomycin, and 0.25 μg/ml amphotericin B at 37°C with 5% CO_2 and 95% humidity. MDCKII cells were seeded on Transwell membrane inserts (6.5-mm diameter, 0.4-μm pore size; Corning Costar, Bodenheim, Germany) at a density of 1.4×10^5 cells per well. After 3 days, medium was replaced with 5 mM sodium butyrate for 24 h before the transport study (Sasaki et al., 2002). The experiments were initiated by replacing the medium on the basal side of the cell layer with Krebs-Henseleiti buffer containing radiolabeled and unlabeled pitavastatin (0.3 μM). The cells were incubated at 37°C, and aliquots of medium were taken from each compartment at designated time points. Radioactivity in 100 μl of medium was measured in a liquid scintillation counter after the addition of scintillation cocktail. At the end of the experiments, the cells were washed three times with 1.5 ml of ice-cold Krebs-Henseleit buffer and solubilized in 500 μl of 0.2 N NaOH. After addition of 100 μl of 1 N HCl, 500-μl aliquots were transferred to scintillation vials. Aliquots (50-μl) of cell lysate were used to determine protein concentrations as described above. To evaluate the efflux transport clearance via recombinant BCRP, MDR1, and MRP2 in the double transfectants, the apparent efflux clearance across the apical membrane (PS_{apical}) was calculated by dividing the steady-state velocity for the transcellular transport ($V_{transcellular}$) of pitavastatin, determined over 3 h, by the intracellular concentration (C_{cell}) of pitavastatin, determined at the end of the experiments (3 h) in the absence or presence of the inhibitors.

$$PS_{apical} = V_{transcellular}/C_{cell} \quad (1)$$

Kinetic Analyses. Ligand uptake in transporter cDNA-transfected cells was expressed as the uptake volume (μl/mg protein), given as the amount of radioactivity associated with the cells (dpm/mg protein) divided by its concentration in the incubation medium (dpm/μl). Transporter-specific uptake was obtained by subtracting the uptake into vector-transfected cells from the uptake into cDNA-transfected cells. Kinetic parameters were obtained using the following equation:

$$v = \frac{V_{max} \times S}{K_m + S} + P_{dif} \times S \quad (2)$$

where v is the uptake velocity of the substrate (pmol/min/mg protein), S is the substrate concentration in the medium (μM), K_m is the Michaelis constant (μM), V_{max} is the maximum uptake rate (pmol/min/mg protein), and P_{dif} is the nonsaturable uptake clearance (μl/min/mg protein). The Damping Gauss-Newton Method algorithm was used with a MULTI program (Yamaoka et al., 1981) to perform nonlinear least-squares data fitting. The input data were weighted as the reciprocal of the observed values. Inhibition constants (K_i) of a series of compounds could be calculated by the following equation, if the substrate concentration was low enough compared with its K_m value.

$$CL(+I) = \frac{CL}{1 + \frac{I}{K_i}} \quad (3)$$

where CL represents the uptake clearance in the absence of inhibitor, $CL(+I)$ represents the uptake clearance in the presence of inhibitor, and I represents the inhibitor concentration. When fitting the data to determine the K_i value, the input data were weighed as the reciprocal of the observed values.

To determine saturable hepatic uptake clearance in human hepatocytes, we first determined the hepatic uptake clearance ($CL_{(2\ min-0.5\ min)}$) (μl/min/10^6 cells) by calculating the slope of the uptake volume (V_d) (μl/10^6 cells) between 0.5 and 2 min as shown previously (Hirano et al., 2004) (eq. 4). The saturable component of the hepatic uptake clearance (CL_{hep}) was determined by subtracting $CL_{(2\ min-0.5\ min)}$ in the presence of 100 μM substrate (excess) from that in the presence of 0.1 μM substrate (tracer) (eq. 5).

$$CL_{(2\ min-0.5\ min)} = \frac{V_{d,2\ min} - V_{d,0.5\ min}}{2 - 0.5} \quad (4)$$

$$CL_{hep} = CL_{(2\ min-0.5\ min),tracer} - CL_{(2\ min-0.5\ min),excess} \quad (5)$$

where $CL_{(2\ min-0.5\ min),tracer}$ and $CL_{(2\ min-0.5\ min),excess}$ represent $CL_{(2\ min-0.5\ min)}$ estimated in the presence of 0.1 and 100 μM substrate, respectively.

Estimation of the Contribution of Transporters to the Hepatic Uptake in Human Hepatocytes by Western Blot Analysis. The ratio of the expression level of each transporter in human hepatocytes (per 10^6 cells) to that in the expression system (per mg protein) was calculated by the intensity of specific bands in Western blot analysis and defined as R_{exp} as shown previously (Hirano et al., 2004). The uptake clearance by each transporter in human hepatocytes was separately calculated by multiplying the uptake clearance of the pitavastatin in transporter-expressing cells (CL_{test}) by R_{exp} as described in the following equation:

$$CL_{hep,test} = CL_{test} \cdot R_{exp} \quad (6)$$

The relative contribution (percentage) of each transporter to the uptake in human hepatocytes was defined by the ratio of $CL_{hep,test}$ for target transporter to that of the sum of $CL_{hep,test}$ for OATP1B1, OATP1B3, and OATP2B1.

Prediction of Clinical DDI between Pitavastatin and Various Drugs via OATP1B1. The degree of inhibition of OATP1B1 in humans was estimated by calculating the following R values, which represent the ratio of the uptake clearance in the absence of inhibitor to that in its presence:

$$R = 1 + \frac{f_u \cdot I_{in,max}}{K_i} \quad (7)$$

where f_u represents the blood unbound fraction of the inhibitor, $I_{in,max}$ represents the estimated maximum inhibitor concentration at the inlet to the liver, and K_i was obtained in the present in vitro study using OATP1B1-expressing HEK293 cells. For the estimation of R value, $I_{in,max}$ was calculated by the method of Ito et al. (1998):

$$I_{in,max} = I_{max} + \frac{F_a \cdot Dose \cdot k_a}{Q_h} \quad (8)$$

where I_{max} represents the reported value for the maximum plasma concentration in the systemic circulation in the clinical situation, F_a represents the absorbed fraction of inhibitor, k_a is the absorption rate constant in the intestine, and Q_h represents the hepatic blood flow rate in humans (1610 ml/min). To estimate the maximum $I_{in,max}$ value, F_a was set at 1, k_a was set at 0.1 min^{-1} [minimum gastric emptying time (10 min)], and the blood-to-plasma concentration ratio was assumed to be 1, if the information from the literature was not available.

Results

Uptake of E_1S and Pitavastatin by OATP2B1-Expressing Cells. The time profiles and Eadie-Hofstee plots of the uptake of E_1S and pitavastatin by OATP2B1-expressing and vector-transfected HEK293 cells are shown in Fig. 1. Pitavastatin as well as E_1S was significantly taken up into OATP2B1-expressing HEK293 cells compared with vector-transfected cells (Fig. 1, A and B). The saturation kinetics of their uptake is shown in Fig. 1, C and D. The concentration dependence of the uptake of E_1S could be explained by a one-saturable component (Fig. 1C). The K_m and V_{max} values for the OATP2B1-mediated uptake of E_1S were 20.9 ± 2.0 μM and 1196 ± 40 pmol/min/mg protein, respectively. The nonsaturable component was observed in the Eadie-Hofstee plot even for the specific uptake of pitavastatin by OATP2B1 (Fig. 1D). The K_m and V_{max} values of pitavastatin for the saturable component and uptake clearance for the nonsaturable component were 1.17 ± 0.28 μM, 7.36 ± 1.43 pmol/min/mg protein, and 2.93 ± 0.16 μl/min/mg protein, respectively. No significant uptake of $E_217\beta G$ by OATP2B1 could be observed (7.51 ± 0.49 and 9.72 ± 1.29 μl/mg protein by vector-transfected and OATP2B1-expressing cells for 5 min, respectively; $n = 3$).

Western Blot Analysis of OATP2B1. The relative expression level of OATP2B1 in crude membrane from transfectants and human hepatocytes was estimated by Western blot analyses. An antiserum against OATP2B1 recognized approximately 85-kDa proteins in the crude membrane fractions prepared from human hepatocytes and OATP2B1-expressing cells (Fig. 2A). The molecular weight of OATP2B1 in human hepatocytes was almost the same as that pre-

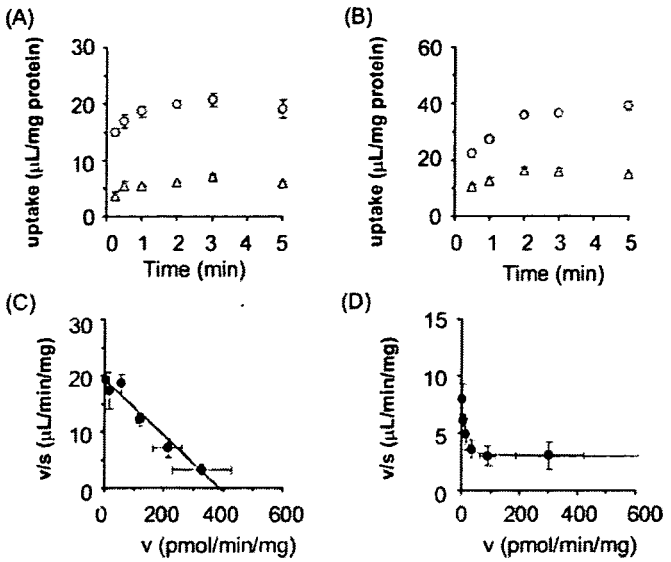

FIG. 1. Time profiles and Eadie-Hofstee plots of the uptake of [^{3}H]E_1S and [^{3}H]pitavastatin by OATP2B1-expressing HEK293 cells. The uptake of 0.1 μM [^{3}H]E_1S (A) and 0.1 μM [^{3}H]pitavastatin (B) by cDNA-transfected cells was examined at 37°C. Open circles and triangles represent the uptake in OATP2B1-expressing HEK293 cells and vector-transfected control cells, respectively. The concentration dependence of OATP2B1-mediated uptake of [^{3}H]E_1S (C) and [^{3}H]pitavastatin (D) is shown as Eadie-Hofstee plots. Closed circles represent the OATP2B1-mediated specific uptake rate, which was obtained by subtracting the initial uptake rate in vector-transfected cells from that in OATP2B1-expressing cells. The initial uptake rate calculated from the uptake of [^{3}H]E_1S and [^{3}H]pitavastatin for 1 and 2 min, respectively, was determined at various concentrations (0.3–100 μM). Solid lines represent the fitted curves obtained by nonlinear regression analysis. Each point represents the mean ± S.E. (n = 3). Where error bars are not shown, the S.E. values are within the limits of the symbol.

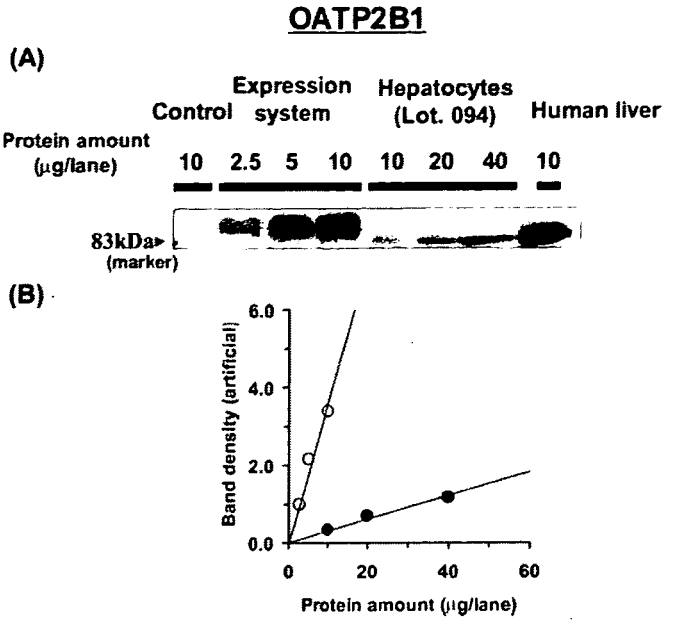

FIG. 2. Western blot analysis of OATP2B1. A, crude membrane fractions (2.5–40 μg) prepared from OATP2B1-expressed HEK293 cells and human hepatocytes (lot 094) were loaded and separated by SDS-polyacrylamide gel electrophoresis (7% separating gel). The sample designated as "Human liver" indicates that the crude membrane vesicles were prepared from a human frozen liver block (lot 020188) as a positive control. OATP2B1 was detected by preimmune antisera raised against the carboxyl terminus of human OATP2B1. B, comparison of the relative expression levels of OATP2B1 between transfectants and hepatocytes is shown. The x and y axes represent the amount of crude membrane obtained from transfectants and human hepatocytes and the intensity of the specific band in Western blot analysis, respectively. Closed circles and open circles indicate the band density of human hepatocytes (lot 094) and OATP2B1-expressing HEK293 cells, respectively. The solid lines represent the fitted lines obtained by linear regression analysis.

pared from human liver block, but was slightly lower than that in OATP2B1-expressing HEK293 cells. No specific band of OATP2B1 was detected in vector-transfected cells. Figure 2B showed the linear relationship between the applied protein amount of crude membrane obtained from OATP2B1-expressing cells and human hepatocytes and the intensity of the specific band measured by digital densitometer. The slope of the regression line in Fig. 2B reflected the relative expression level of OATP2B1 in transfectants and hepatocytes.

Estimation of Contribution of OATP1B1, OATP1B3, and OATP2B1 in Human Hepatocytes by Western Blot Analysis. We calculated the estimated uptake clearance of pitavastatin by OATP1B1, OATP1B3, and OATP2B1 in human hepatocytes by the relative expression level of each transporter (Table 1). We obtained 62.1 μg of protein in crude membrane from 1 mg of whole cell protein in OATP2B1-expressing HEK293 cells, whereas 178, 89, and 82 μg of protein were obtained in crude membrane from 10^6 human hepatocytes of lot OCF, 094, and ETR, respectively. When the band density per unit protein amount in crude membrane of OATP2B1-expressing HEK293 cells is defined as 1, the relative expression levels of OATP2B1 per unit protein amount in crude membrane of hepatocytes of lots OCF, 094, and ETR are 0.200, 0.152, and 0.112 (per microgram), respectively. Using these R_{exp} values and our previous results (Hirano et al., 2004; shown in Table 1), we estimated the relative contribution of OATP1B1, OATP1B3, and OATP2B1 to the hepatic uptake of pitavastatin in human hepatocytes.

Inhibitory Effects of $E_2$17βG and E_1S on the Uptake of Pitavastatin by Transporter-Expression System and Human Hepatocytes. Inhibitory effects of $E_2$17βG and E_1S on the uptake of pitavastatin were examined by human cryopreserved hepatocytes (Fig. 3). $E_2$17βG (100 μM) inhibited OATP1B1- and OATP1B3-mediated transport of pitavastatin to 10.0 ± 3.2 and 21.7 ± 8.7% of control, respectively (n = 3), whereas OATP2B1-mediated transport was not affected by 100 μM $E_2$17βG (91.8 ± 16.6%). In contrast, 100 μM E_1S inhibited OATP1B1- and OATP2B1-mediated transport of pitavastatin to 7.19 ± 2.94 and 56.5 ± 3.2% of control, respectively (n = 3), whereas OATP1B3-mediated transport was not affected by 100 μM E_1S (102 ± 7%). In three batches of human hepatocytes, pitavastatin uptake was almost inhibited by 100 μM $E_2$17βG (Fig. 3A) and E_1S (Fig. 3B).

Prediction of DDI between Pitavastatin and Various Compounds by OATP1B1-Expressing HEK293 Cells. To identify clinically relevant inhibitors for OATP1B1-mediated pitavastatin uptake, inhibitory effects of several compounds on the uptake of pitavastatin were determined by OATP1B1-expressing cells. These compounds include therapeutic agents that were reported to cause DDI with statins (Williams and Feely, 2002). Cyclosporin A, fenofibrate, gemfibrozil, and gemfibrozil metabolites (gemfibrozil-M3 and gemfibrozil-1-*O*-glucuronide) were also investigated because drug interaction studies with pitavastatin have been previously reported (Hasunuma et al., 2003; Mathew et al., 2004). Most of the compounds we tested could inhibit OATP1B1-mediated pitavastatin uptake (Table 2). We also obtained the blood unbound fraction (f_u) and calculated the estimated maximum concentration at the inlet to the liver ($I_{in,max}$) of the inhibitors from the literature information (Clark et al., 1992; Hardman et al., 2001; package insert of each drug). Inhibition constants (K_i) of various compounds for OATP1B1 obtained in the present study and the ratio of the uptake clearance in the absence of inhibitor to that in its presence (R value) are summarized in Table 2. R values of cyclosporin A, rifampicin, rifamycin SV, clarithromycin,

TABLE 1

Contribution of OATP1B1, OATP1B3, and OATP2B1 to the hepatic uptake of pitavastatin determined by the relative expression level

Hepatocyte Lot	Ratio of Expression Level[a] (Hepatocyte/Expression System)			Estimated Clearance[b]		
	$R_{exp,OATP1B1}$	$R_{exp,OATP1B3}$	$R_{exp,OATP2B1}$	OATP1B1	OATP1B3	OATP2B1
					μl/min/10⁶ cells	
OCF	2.90[c]	1.21[c]	0.200	222	37.0	0.658
				85.5%	14.3%	0.253%
094	1.58[c]	0.930[c]	0.152	121	28.5	0.500
				80.7%	19.0%	0.333%
ETR	0.890[c]	0.737[c]	0.112	68.2	22.6	0.368
				74.8%	24.8%	0.405%

[a] Ratio of the expression level was determined by the intensity of the specific band in the crude membrane prepared from human hepatocytes (per 10^6 cells) divided by that in the crude membrane from transporter-expressing cells (per milligram) in Western blot analysis.

[b] In the 'Estimated Clearance' column, each percentage value indicates the percentage of the OATP1B1-, OATP1B3-, or OATP2B1-mediated uptake clearance relative to the sum of the estimated clearance mediated by OATP1B1, OATP1B3, and OATP2B1. The details of this estimation are described under *Materials and Methods*.

[c] Values from Hirano et al. (2004).

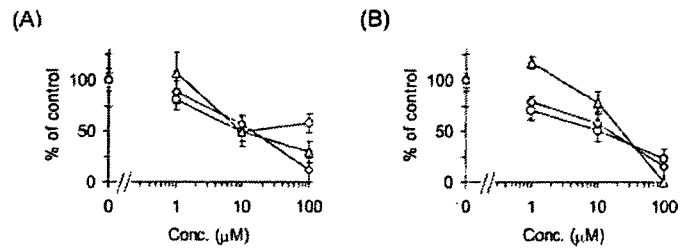

FIG. 3. Inhibitory effects of $E_2 17\beta G$ and $E_1 S$ on the uptake of [^{3}H]pitavastatin by human hepatocytes. The transport of [^{3}H]pitavastatin (0.1 μM) into human hepatocytes was determined in the presence or absence of $E_2 17\beta G$ (A) and $E_1 S$ (B) at the designated concentrations. Open circles, triangles, and squares represent the uptake in human hepatocytes of lots OCF, 094, and ETR, respectively. The detailed method for calculation of the uptake clearance in hepatocytes (CL_{hep}) is described under *Materials and Methods*. The values are expressed as a percentage of the uptake of [^{3}H]pitavastatin in the absence of inhibitors. Each point represents the mean ± S.E. (n = 3).

and indinavir were higher than 2.5, suggesting that these drugs can interact with pitavastatin in a clinical situation.

Inhibitory Effects of Cyclosporin A, Gemfibrozil, and Its Metabolites on the Transcellular Transport of Pitavastatin in OATP1B1/MRP2, OATP1B1/MDR1, and OATP1B1/BCRP Double Transfectants. The inhibitory effects of cyclosporin A, gemfibrozil, gemfibrozil-1-*O*-glucuronide, and gemfibrozil-M3 on the transcellular transport of pitavastatin were investigated in double-transfected cells. The transcellular transport clearance (PS_{net}) of pitavastatin was drastically decreased by cyclosporin A in all kinds of double transfectants (Fig. 4A). The efflux clearance from cells to the apical compartment (PS_{apical}) was also potently reduced by cyclosporin A (Fig. 5A). In contrast, gemfibrozil and gemfibrozil-1-*O*-glucuronide did not change either PS_{net} or PS_{apical} up to 100 μM (Figs. 4 and 5). Gemfibrozil-M3 (300 μM) could not inhibit the PS_{apical} of pitavastatin in OATP1B1/BCRP-, OATP1B1/MDR1-, and OATP1B1/MRP2-expressing MDCKII cells (data not shown). The K_i values of these inhibitors on the PS_{net} and PS_{apical} of pitavastatin are summarized in Table 3.

TABLE 2

The K_i values for OATP1B1-mediated pitavastatin uptake and the prediction of the possibility of DDI by considering the maximum plasma unbound concentration at the inlet to the liver

The K_i values are expressed as mean ± computer-calculated S.D. R value = $1 + f_u \cdot I_{in,max}/K_i$.

Inhibitor	K_i Value for OATP1B1	R Value
	μM	
Cyclosporin A	0.242 ± 0.029	3.55
Tacrolimus	0.611 ± 0.069	1.20
Rifampicin	0.477 ± 0.030	13.4
Rifamycin SV	0.171 ± 0.024	65.6
Tolbutamide	>100	<1.21
Glibenclamide	0.746 ± 0.101	1.00
Fluconazole	>100	<1.25
Ketoconazole	19.2 ± 3.9	1.03
Itraconazole	>100	<1.00
Gemfibrozil	25.2 ± 4.7	1.08
Gemfibrozil-1-*O*-glucuronide	22.6 ± 5.8	1.10[a]
Gemfibrozil-M3	>300	<1.03[a]
Clofibrate	>300	<1.03
Ciprofibrate	141 ± 22	1.01
Bezafibrate	68.6 ± 11.9	1.03
Fenofibrate	>300	<1.00
Cimetidine	>300	<1.14
Ranitidine	>300	<1.16
Valsartan	8.96 ± 1.33	1.10
Telmisartan	0.436 ± 0.043	1.16
Chlorzoxazone	>100	<1.00
Colchichine	>100	<1.07
Phenytoin	>100	<1.03
Clarithromycin	8.26 ± 0.54	3.29
Erythromycin	11.4 ± 2.1	1.25
Indinavir	18.4 ± 1.9	2.77
Ritonavir	0.781 ± 0.048	2.25
Saquinavir	1.59 ± 0.13	1.62
Probenecid	76.2 ± 7.1	1.85
Methotrexate	>300	<1.01
Digoxin	31.7 ± 3.0	1.00
Diltiazem	>100	<1.03
Verapamil	51.6 ± 15.9	1.02
Warfarin	83.3 ± 9.7	1.00

[a] These values were calculated by using the reported values for the maximum plasma concentration of inhibitors in the clinical situations, instead of $I_{in,max}$, because we did not have enough parameters to estimate the $I_{in,max}$ value.

Discussion

In the present study, we have excluded the possibility of a major contribution of OATP2B1 to the hepatic uptake of pitavastatin and confirmed that OATP1B1 is the most important transporter for its uptake. Next, the inhibitory effects of pitavastatin uptake by several drugs in OATP1B1-expressing cells were also investigated, and we discussed the possibility of DDI in clinical stage by considering the inhibition constant (K_i) obtained from in vitro analysis and the estimated maximum unbound concentration of each inhibitor at the inlet to the liver.

We observed the significant saturable uptake of pitavastatin in OATP2B1-expressing cells compared with control cells at pH 7.4 with a K_m value of 1.17 μM (Fig. 1). It has been shown that specific uptake of pravastatin by OATP2B1 was not significantly observed at pH 7.4, whereas it can be transported at pH 5.0 (Nozawa et al., 2004), indicating that pitavastatin is preferentially recognized by OATP2B1

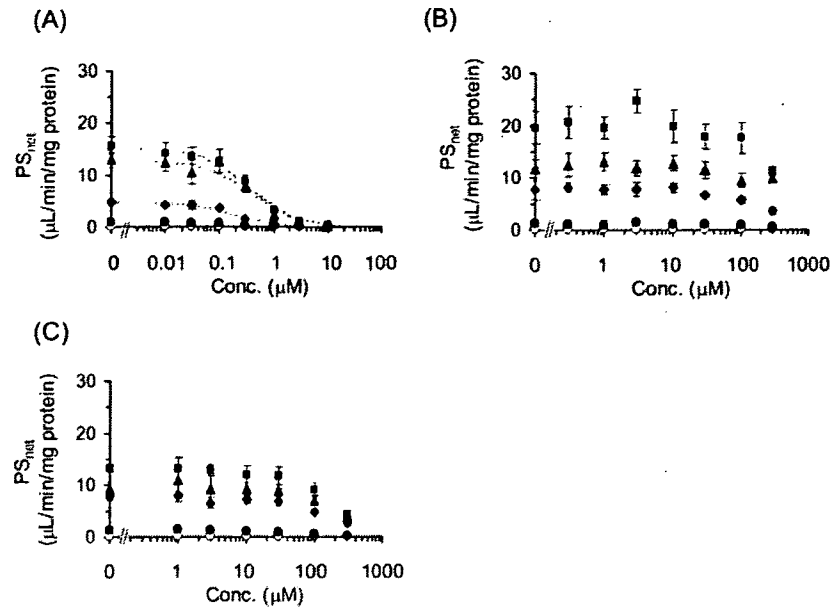

FIG. 4. Inhibitory effects of cyclosporin A, gemfibrozil, and gemfibrozil-1-*O*-glucuronide on the transcellular transport of [^{3}H]pitavastatin. The basal-to-apical flux of [^{3}H]pitavastatin (0.3 μM) across MDCKII monolayer expressing OATP1B1 (closed circles), OATP1B1/BCRP (closed diamonds), OATP1B1/MDR1 (closed squares), and OATP1B1/MRP2 (closed triangles) was determined compared with vector-transfected control cells (open circles) in the absence and presence of cyclosporin A (A), gemfibrozil (B), or gemfibrozil-1-*O*-glucuronide (C). The *x* and *y* axes represent the concentration of each inhibitor in the medium at the basal compartment and the transport clearance for the transcellular transport (PS_{net}) of [^{3}H]pitavastatin (μl/min/mg protein). Each point and vertical bar represent the mean ± S.E. of three determinations. Where vertical bars are not shown, the S.E. values are within the limits of the symbol. Dotted lines represent the fitted curves obtained by nonlinear regression analysis.

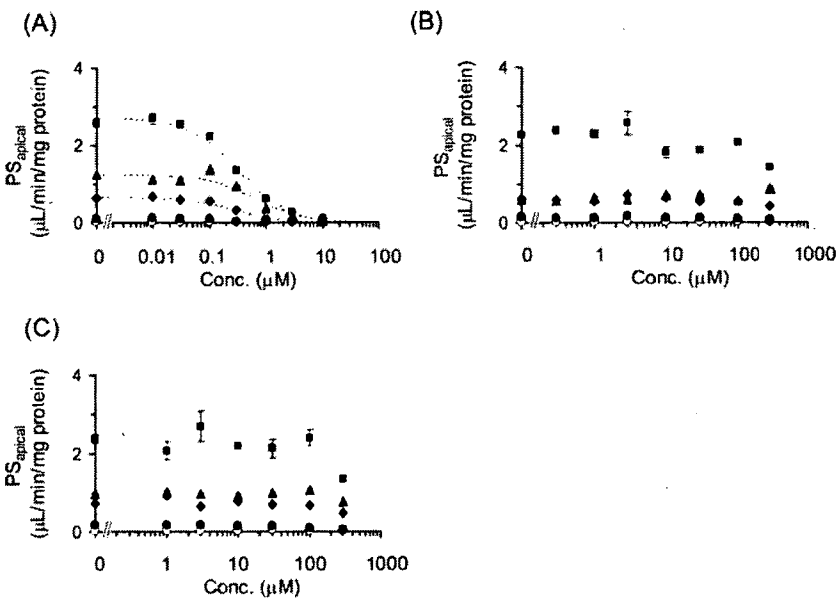

FIG. 5. Inhibitory effects of cyclosporin A, gemfibrozil, and gemfibrozil-1-*O*-glucuronide on the efflux transport of [^{3}H]pitavastatin across the apical membrane of MDCKII cells. The efflux transport clearance of [^{3}H]pitavastatin (0.3 μM) across the apical membrane (PS_{apical}) of MDCKII monolayer expressing OATP1B1 (closed circles), OATP1B1/BCRP (closed diamonds), OATP1B1/MDR1 (closed squares), and OATP1B1/MRP2 (closed triangles) was determined compared with vector-transfected control cells (open circles) in the absence and presence of cyclosporin A (A), gemfibrozil (B), or gemfibrozil-1-*O*-glucuronide (C). The *x* and *y* axes represent the concentration of each inhibitor in the medium at the basal compartment and the transport clearance for the efflux transport across the apical membrane (PS_{apical}) of [^{3}H]pitavastatin (μl/min/mg protein). Each point and vertical bar represents the mean ± S.E. of three determinations. Where vertical bars are not shown, the S.E. values are within the limits of the symbol. Dotted lines represent the fitted curves obtained by nonlinear regression analysis.

compared with pravastatin. The K_m value of E_1S for OATP2B1 from our analyses was 20.9 μM (Fig. 1), which was almost comparable to the reported values (Kullak-Ublick et al., 2001; Nozawa et al., 2004), whereas the significant uptake of $E_2 17\beta G$ at pH 7.4 was not detected as described previously (Kullak-Ublick et al., 2001; Nozawa et al., 2004).

Then, to refute the possibility that OATP2B1 plays an important role in the pitavastatin uptake in human hepatocytes and confirm the major contribution of OATP1B1, we took two strategies: 1) to check the inhibitable portion of pitavastatin uptake by two inhibitors in human hepatocytes, and 2) to compare the relative expression level of OATP2B1 in human hepatocytes and OATP2B1-expressing cells by Western blot analysis. As a result of the first approach, pitavastatin uptake in human hepatocytes was almost completely suppressed

TABLE 3

The K_i values of cyclosporin A, gemfibrozil, and gemfibrozil-1-O-glucuronide for the PS_{net} and PS_{apical} of pitavastatin in double-transfected cells

The values are expressed as mean ± computer-calculated S.D.

Transfectants	Cyclosporin A	Gemfibrozil	Gemfibrozil-1-*O*-glucuronide
PS_{net} (K_i, μM)			
OATP1B1/BCRP	0.194 ± 0.048	>100	>100
OATP1B1/MDR1	0.359 ± 0.046	>100	>100
OATP1B1/MRP2	0.407 ± 0.132	>100	>100
PS_{apical} (K_i, μM)			
OATP1B1/BCRP	0.273 ± 0.083	>300	>300
OATP1B1/MDR1	0.330 ± 0.037	>300	>300
OATP1B1/MRP2	0.662 ± 0.252	>300	>300

by both 100 μM $E_2$17βG (inhibitor of OATP1B1/OATP1B3) and E_1S (inhibitor of OATP1B1/OATP2B1) (Fig. 3), suggesting that OATP1B1 mainly contributes to the hepatic uptake of pitavastatin. In contrast, the uptake of telmisartan, which can be accepted by OATP1B3, but not OATP1B1, into human hepatocytes could not be inhibited by 100 μM E_1S (Ishiguro et al., 2006), supporting the validity of our approach. Moreover, from the comparison of the expression level of OATP2B1 between transfectants and hepatocytes by Western blot analysis (Fig. 2), we could calculate the OATP1B1-, OATP1B3-, and OATP2B1-mediated uptake into hepatocytes by multiplying the uptake clearance of pitavastatin in the expression system by the ratio of the expression level in these cells (R_{exp}). The results indicated that the contribution of OATP2B1 to the hepatic uptake of pitavastatin was less than 1%, although it is a substrate of OATP2B1, and that OATP1B1 is the most important in the hepatic uptake of pitavastatin, which is consistent with the previous results calculated from other approaches (Hirano et al., 2004).

Pitavastatin is mainly eliminated from liver in an unchanged form (Kojima et al., 2001). From the pharmacokinetic point of view, the change in the hepatic uptake clearance always directly affects the overall hepatic clearance for this type of drug (Shitara et al., 2005). Since we clarified that pitavastatin is taken up into the hepatocytes mainly by OATP1B1 in the present study, we focused on the inhibitory effects of various drugs on the OATP1B1-mediated uptake of pitavastatin. The combination therapy of statins and various drugs, such as fibrates, immune suppressants, antidiabetic drugs, antihypertensive drugs, and antibiotics, is widely used in the clinical situation (Williams and Feely, 2002). It has been reported that the plasma area under the plasma concentration-time curve of several statins was increased by coadministration of cyclosporin A and gemfibrozil (Shitara et al., 2005). Recently, Shitara et al. (2003) have demonstrated that inhibition of OATP1B1 is a major mechanism of DDI between cerivastatin and cyclosporin A. Campbell et al. (2004) also suggested that unconjugated hyperbilirubinemia induced by indinavir, rifamycin SV, and cyclosporin A is partly caused by the inhibition of OATP1B1-mediated uptake. Although pitavastatin uptake could be inhibited by several drugs in in vitro experiments, from the results of our calculation (Ito et al., 1998), the R values of most of the drugs we tested are almost equal to 1 (Table 2). To avoid the false-negative prediction of DDI, we estimated the inhibitory effects of the maximum plasma unbound concentration of inhibitors at the inlet to the liver ($I_{in,max}$). Therefore, it is unlikely that the OATP1B1-mediated DDI between pitavastatin and these drugs occurs in the clinical stage. However, we should pay attention to the OATP1B1-mediated DDI for pitavastatin with coadministration of cyclosporin A, rifampicin, rifamycin SV, clarithromycin, and indinavir because their R values exceeded 2.5 (Table 2), although the degree of the inhibition could be overestimated. We should notice that these drugs may also cause DDI with compounds that are mainly eliminated from liver via OATP1B1, including other statins. The previous clinical studies have shown that plasma concentration of pitavastatin was increased by cyclosporin A (Hasunuma et al., 2003), but not gemfibrozil and fenofibrate (Mathew et al., 2004). This evidence was consistent with our prediction (Table 2).

Conversely, gemfibrozil caused an increase in plasma concentration of cerivastatin (Backman et al., 2002). One of the major mechanisms of DDI between cerivastatin and gemfibrozil was considered to be the inhibition of CYP2C8-mediated metabolism of cerivastatin by gemfibrozil-1-*O*-glucuronide, which is thought to be concentrated in hepatocytes (Shitara et al., 2004). Gemfibrozil is metabolized into M3 and its glucuronide in the liver. Therefore, to investigate whether gemfibrozil, gemfibrozil-M3, and gemfibrozil-1-*O*-glucuronide could affect the transcellular transport by the inhibition of efflux transporter in liver, we checked their inhibitory effects on transcellular transport clearance (PS_{net}) and efflux clearance (PS_{apical}) in double-transfected cells. As a result, gemfibrozil and its metabolites could not inhibit the efflux transporters and affect transcellular transport, whereas cyclosporin A strongly inhibited both PS_{net} and PS_{apical} in all kinds of double-transfected cells (Figs. 4 and 5). This result suggested that the DDI between cyclosporin A and pitavastatin may be caused not only by the inhibition of OATP1B1-mediated uptake, but also by the inhibition of efflux transport mediated by MRP2, MDR1, and BCRP.

In conclusion, we have confirmed the major contribution of OATP1B1 to the hepatic uptake of pitavastatin in human hepatocytes. In addition, focusing on OATP1B1, inhibitory effects of various drugs on pitavastatin uptake were determined by OATP1B1-expressing cells, and its clinical relevance was discussed by considering the R values. Our results suggested that OATP1B1-mediated DDI between pitavastatin and some drugs indicated above may be clinically relevant and should be taken notice of during coadministration of inhibitors of OATP1B1.

Acknowledgments. We thank Dr. Piet Borst (The Netherlands Cancer Institutes, Amsterdam, The Netherlands) for providing the MDCKII cells expressing MRP2 and MDR1, Dr. Yoshihiro Miwa (University of Tsukuba, Japan) for providing pEB6CAGMCS/SRZeo vector, and Ying Tian and Miyuki Kambara for the construction of OATP2B1-expressing cells. We also thank Kowa Co. Ltd. (Tokyo, Japan) for providing radiolabeled pitavastatin and unlabeled pitavastatin, and Sankyo Co., Ltd. (Tokyo, Japan) and Chemtech Labo. Inc. (Tokyo, Japan) for providing gemfibrozil-1-*O*-glucuronide.

References

Aoki T, Nishimura H, Nakagawa S, Kojima J, Suzuki H, Tamaki T, Wada Y, Yokoo N, Sato F, Kimata H, et al. (1997) Pharmacological profile of a novel synthetic inhibitor of 3-hydroxy-3-methylglutaryl-coenzyme A reductase. *Arzneim-Forsch* **47**:904–909.

Backman JT, Kyrklund C, Neuvonen M, and Neuvonen PJ (2002) Gemfibrozil greatly increases plasma concentrations of cerivastatin. *Clin Pharmacol Ther* **72**:685–691.

Campbell SD, de Morais SM, and Xu JJ (2004) Inhibition of human organic anion transporting polypeptide OATP1B1 as a mechanism of drug-induced hyperbilirubinemia. *Chem-Biol Interact* **150**:179–187.

Clark WG, Brater DC, Johnson AR, and Goth A (1992) *Goth's Medical Pharmacology*, 13th ed, Mosby-Year Book, St. Louis.

Evans M and Rees A (2002) Effects of HMG-CoA reductase inhibitors on skeletal muscle: are all statins the same? *Drug Saf* **25**:649–663.

Hagenbuch B and Meier PJ (2003) The superfamily of organic anion transporting polypeptides. *Biochim Biophys Acta* **1609**:1–18.

Hardman J, Limbird L, and Gilman AG (2001) *Goodman and Gilman's The Pharmacological Basis of Therapeutics*, 9th ed, McGraw-Hill, New York.

Hasunuma T, Nakamura M, Yachi T, Arisawa N, Fukushima K, Iijima H, and Saito Y (2003) The drug-drug interactions of pitavastatin (NK-104), a novel HMG-CoA reductase inhibitor and cyclosporine. *J Clin Ther Med* **19**:381–389.

Hirano M, Maeda K, Shitara Y, and Sugiyama Y (2004) Contribution of OATP2 (OATP1B1) and OATP8 (OATP1B3) to the hepatic uptake of pitavastatin in humans. *J Pharmacol Exp Ther* **311**:139–146.

Ichimaru N, Takahara S, Kokado Y, Wang JD, Hatori M, Kameoka H, Inoue T, and Okuyama A (2001) Changes in lipid metabolism and effect of simvastatin in renal transplant recipients induced by cyclosporine or tacrolimus. *Atherosclerosis* **158**:417–423.

Ishiguro N, Maeda K, Kishimoto W, Saito A, Harada A, Ebner T, Roth W, Igarashi T, and Sugiyama Y (2006) Predominant contribution of OATP1B3 to the hepatic uptake of telmisartan, an angiotensin II receptor antagonist, in humans. *Drug Metab Dispos* **34**:1109–1115.

Ito K, Iwatsubo T, Kanamitsu S, Ueda K, Suzuki H, and Sugiyama Y (1998) Prediction of pharmacokinetic alterations caused by drug-drug interactions: metabolic interaction in the liver. *Pharmacol Rev* **50**:387–412.

Kajinami K, Takekoshi N, and Saito Y (2003) Pitavastatin: efficacy and safety profiles of a novel synthetic HMG-CoA reductase inhibitor. *Cardiovasc Drug Rev* **21**:199–215.

Kantola T, Kivisto KT, and Neuvonen PJ (1998) Erythromycin and verapamil considerably increase serum simvastatin and simvastatin acid concentrations. *Clin Pharmacol Ther* **64**:177–182.

Kimata H, Fujino H, Koide T, Yamada Y, Tsunenari Y, Yonemitsu M, and Yanagawa Y (1998) Studies on the metabolic fate of NK-104, a new inhibitor of HMG-CoA reductase: I. Absorption, distribution, metabolism and excretion in rats. *Xenobiol Metab Dispos* **13**:484–498.

Kobayashi D, Nozawa T, Imai K, Nezu J, Tsuji A, and Tamai I (2003) Involvement of human organic anion transporting polypeptide OATP-B (SLC21A9) in pH-dependent transport across intestinal apical membrane. *J Pharmacol Exp Ther* **306**:703–708.

Kojima J, Ohshima T, Yoneda M, and Sawada H (2001) Effect of biliary excretion on the pharmacokinetics of pitavastatin (NK-104) in dogs. *Xenobio Metab Dispos* **16**:497–502.

Kullak-Ublick GA, Ismair MG, Stieger B, Landmann L, Huber R, Pizzagalli F, Fattinger K, Meier PJ, and Hagenbuch B (2001) Organic anion-transporting polypeptide B (OATP-B) and its functional comparison with three other OATPs of human liver. *Gastroenterology* **120**:525–533.

Lowry OH, Rosebrough NJ, Farr AL, and Randall RJ (1951) Protein measurement with the Folin phenol reagent. *J Biol Chem* **193**:265–267

Mathew P, Cuddy T, Tracewell WG, and Salazar D (2004) An open-label study on the pharmacokinetics (PK) of pitavastatin (NK-104) when administered concomitantly with fenofibrate or gemfibrozil in healthy volunteers. *Clin Pharmacol Ther* **75**:33.

Matsushima S, Maeda K, Kondo C, Hirano M, Sasaki M, Suzuki H, and Sugiyama Y (2005) Identification of the hepatic efflux transporters of organic anions using double transfected MDCKII cells expressing human OATP1B1/MRP2, OATP1B1/MDR1 and OATP1B1/BCRP. *J Pharmacol Exp Ther* **314**:1059–1067.

Mizuno N, Niwa T, Yotsumoto Y, and Sugiyama Y (2003) Impact of drug transporter studies on drug discovery and development. *Pharmacol Rev* **55**:425–461.

Neuvonen PJ, Kantola T, and Kivisto KT (1998) Simvastatin but not pravastatin is very susceptible to interaction with the CYP3A4 inhibitor itraconazole. *Clin Pharmacol Ther* **63**:332–341.

Nozawa T, Imai K, Nezu J, Tsuji A, and Tamai I (2004) Functional characterization of pH-sensitive organic anion transporting polypeptide OATP-B in human. *J Pharmacol Exp Ther* **308**:438–445.

Olbricht C, Wanner C, Eisenhauer T, Kliem V, Doll R, Boddaert M, O'Grady P, Krekler M, Mangold B, and Christians U (1997) Accumulation of lovastatin, but not pravastatin, in the blood of cyclosporine-treated kidney graft patients after multiple doses. *Clin Pharmacol Ther* **62**:311–321.

Sasaki M, Suzuki H, Ito K, Abe T, and Sugiyama Y (2002) Transcellular transport of organic anions across a double-transfected Madin-Darby canine kidney II cell monolayer expressing both human organic anion-transporting polypeptide (OATP2/SLC21A6) and Multidrug resistance-associated protein 2 (MRP2/ABCC2). *J Biol Chem* **277**:6497–6503.

Shimizu M, Fuse K, Okudaira K, Nishigaki R, Maeda K, Kusuhara H, and Sugiyama Y (2005) Contribution of OATP (organic anion-transporting polypeptide) family transporters to the hepatic uptake of fexofenadine in humans. *Drug Metab Dispos* **33**:1477–1481.

Shitara Y, Hirano M, Sato H, and Sugiyama Y (2004) Gemfibrozil and its glucuronide inhibit the organic anion transporting polypeptide 2 (OATP2/OATP1B1:SLC21A6)-mediated hepatic uptake and CYP2C8-mediated metabolism of cerivastatin: analysis of the mechanism of the clinically relevant drug-drug interaction between cerivastatin and gemfibrozil. *J Pharmacol Exp Ther* **311**:228–236.

Shitara Y, Itoh T, Sato H, Li AP, and Sugiyama Y (2003) Inhibition of transporter-mediated hepatic uptake as a mechanism for drug-drug interaction between cerivastatin and cyclosporin A. *J Pharmacol Exp Ther* **304**:610–616.

Shitara Y, Sato H, and Sugiyama Y (2005) Evaluation of drug-drug interaction in the hepatobiliary and renal transport of drugs. *Annu Rev Pharmacol Toxicol* **45**:689–723.

Simonson SG, Raza A, Martin PD, Mitchell PD, Jarcho JA, Brown CD, Windass AS, and Schneck DW (2004) Rosuvastatin pharmacokinetics in heart transplant recipients administered an antirejection regimen including cyclosporine. *Clin Pharmacol Ther* **76**:167–177.

Sugiyama D, Kusuhara H, Shitara Y, Abe T, Meier PJ, Sekine T, Endou H, Suzuki H, and Sugiyama Y (2001) Characterization of the efflux transport of 17beta-estradiol-D-17beta-glucuronide from the brain across the blood-brain barrier. *J Pharmacol Exp Ther* **298**:316–322.

Tamai I, Nozawa T, Koshida M, Nezu J, Sai Y, and Tsuji A (2001) Functional characterization of human organic anion transporting polypeptide B (OATP-B) in comparison with liver-specific OATP-C. *Pharm Res (NY)* **18**:1262–1269.

Williams D and Feely J (2002) Pharmacokinetic-pharmacodynamic drug interactions with HMG-CoA reductase inhibitors. *Clin Pharmacokinet* **41**:343–370.

Yamaoka K, Tanigawara Y, Nakagawa T, and Uno T (1981) A pharmacokinetic analysis program (MULTI) for microcomputer. *J Pharmacobio-Dyn* **4**:879–885.

Address correspondence to: Dr. Yuichi Sugiyama, Department of Molecular Pharmacokinetics, Graduate School of Pharmaceutical Sciences, The University of Tokyo, 7-3-1 Hongo, Bunkyo-ku, Tokyo, 113-0033 Japan. E-mail: sugiyama@mol.f.u-tokyo.ac.jp

0090-9556/06/3407-1109–1115$20.00
DRUG METABOLISM AND DISPOSITION
Copyright © 2006 by The American Society for Pharmacology and Experimental Therapeutics
DMD 34:1109–1115, 2006

Vol. 34, No. 7
9175/3119866
Printed in U.S.A.

PREDOMINANT CONTRIBUTION OF OATP1B3 TO THE HEPATIC UPTAKE OF TELMISARTAN, AN ANGIOTENSIN II RECEPTOR ANTAGONIST, IN HUMANS

Naoki Ishiguro, Kazuya Maeda, Wataru Kishimoto, Asami Saito, Akiko Harada, Thomas Ebner, Willy Roth, Takashi Igarashi, and Yuichi Sugiyama

Department of Pharmacokinetics and Non-Clinical Safety, Kawanishi Pharma Research Institute, Nippon Boehringer Ingelheim Co., Ltd., Hyogo, Japan (N.I., W.K., A.S., A.H., T.I.); Department of Molecular Pharmacokinetics, Graduate School of Pharmaceutical Sciences, the University of Tokyo, Tokyo, Japan (K.M., Y.S.); and Department of Pharmacokinetics and Drug Metabolism, Boehringer Ingelheim Pharma KG, Biberach on der Riss, Germany (T.E., W.R.)

ABSTRACT:

Telmisartan, a nonpeptide angiotensin II receptor antagonist, is selectively distributed to liver. In the present study, we have characterized the contribution of organic anion transporting polypeptide (OATP) isoforms to the hepatic uptake of telmisartan by isolated rat hepatocytes, human cryopreserved hepatocytes, and human transporter-expressing cells. Because it is difficult to evaluate the transport activity of telmisartan because of its extensive adsorption to cells and culture materials, we performed the uptake study in the presence of human serum albumin. The saturable uptake of telmisartan into isolated rat hepatocytes took place in a Na^+-independent manner and was inhibited by pravastatin, taurocholate, and digoxin, which are Oatp substrates and inhibitors, but not by organic cation, tetraethylammonium, indicating the involvement of Oatp isoforms in its uptake into rat hepatocytes. To identify which human OATP transporters are important for the hepatic uptake of telmisartan, the uptake assay was carried out using OATP1B1- and OATP1B3-expressing human embryonic kidney 293 cells and cryopreserved human hepatocytes. The uptake of telmisartan by OATP1B3-expressing cells was saturable (K_m = 0.81 μM) and significantly higher than that by vector-transfected cells. In contrast, no significant uptake was observed in OATP1B1-expressing cells. We also observed the saturable uptake of telmisartan by human hepatocytes. Thirty micromolar estrone-3-sulfate, which can selectively inhibit OATP1B1-mediated uptake compared with OATP1B3, did not inhibit the uptake of telmisartan in human hepatocytes, whereas it could inhibit the uptake of estradiol 17β-D-glucuronide mediated by OATP1B1. These results suggest that OATP1B3 is predominantly involved in the hepatic uptake of telmisartan in humans.

The renin-angiotensin-aldosterone system plays a central role in blood pressure regulation (Hedner, 1999). This system leads to the production of the hormone angiotensin I, which is converted to the active hormone angiotensin II by angiotensin-converting enzyme. Angiotensin II receptor antagonists prevent angiotensin II from exerting its vasoconstrictive effects on blood vessels (Oliverio and Coffman, 1997). Five nonpeptide angiotensin receptor antagonists, losartan, candesartan cilexetil, valsartan, telmisartan, and olmesartan medoxomil, are commercially available in Japan. Losartan, candesartan cilexetil, and olmesartan medoxomil are prodrugs, whereas valsartan and telmisartan are themselves pharmacologically active. All of them are mainly excreted into feces from the liver.

Telmisartan (Fig. 1) is a lipophilic compound with a log *P* value of 3.2, and it exists in anionic form at neutral pH (Wienen et al., 2000). Telmisartan is metabolized to an inactive acylglucuronide conjugate by UDP-glucuronosyltransferases in the intestinal wall and liver (Stangier et al., 2000c). The acylglucuronide is rapidly excreted into the bile and accounts for 10% of the circulating drug-related material 1 h after p.o. administration of telmisartan (Stangier et al., 2000a,c). Telmisartan is selectively distributed to the liver in rats with a liver/plasma concentration ratio of more than 40 (Wienen et al., 2000). After a single p.o. and i.v. administration in humans, more than 98% of the total radioactivity was recovered in feces as a parent drug, and less than 1% of the radioactivity was recovered in urine (Stangier et al., 2000a). Telmisartan shows a large interindividual variability in its plasma concentrations, and both the maximum concentration in plasma (C_{max}) and area under the plasma concentration-time curve (AUC) increased in a slightly more than the dose-proportional manner after p.o. administration (Stangier et al., 2000a,c). Because liver is a major clearance organ of telmisartan, it is essential to assess the uptake mechanism of telmisartan by human hepatocytes to gain an insight into the mechanism for its nonlinear pharmacokinetics and large interindividual variability.

Several transporters, such as Na^+-taurocholate cotransporting polypeptide and organic anion transporting polypeptide (OATP) 1B1 (previously called OATP-C/OATP2/LST-1), OATP1B3 (previously called OATP8/LST-2), OATP2B1 (previously called OATP-B), organic anion transporter 2, and organic cation transporter 1, are ex-

This work was supported in part by a Health and Labor Sciences Research Grants from Ministry of Health, Labor, and Welfare for the Research on Advanced Medical Technology and Grant-in Aid for Young Scientists (B) (17790113) from the Ministry of Education, Culture, Sports, Science, and Technology.

Article, publication date, and citation information can be found at http://dmd.aspetjournals.org.

doi:10.1124/dmd.105.009175.

ABBREVIATIONS: AUC, area under the plasma concentration-time curve; OATP, organic anion transporting polypeptide; $E_2$17βG, estradiol 17β-D-glucuronide; CCK-8, cholecystokinin octapeptide; E-sul, estrone-3-sulfate; TEA, tetraethylammonium; HEK, human embryonic kidney; HSA, human serum albumin.